PROC. 19th **INT. CONF. HIGH ENERGY PHYSICS**
TOKYO, 1978

P 6 Experimental Review of Electron, Muon and Photon Physics

E. GABATHULER

CERN

Introduction

In order to review in a one-hour talk the work of many experiments in the field of photon, electron and muon physics, it has been necessary to be selective and to apologise to all those groups whose work is not reported in this plenary review. However, there have been many excellent mini-reviews in the parallel sessions of this Conference and much more detailed information can be found there as well as in previous Conference reports.[1]

For the study of hadronic final states, the photon can be considered as a real or virtual probe, and there is now considerable evidence that the dual role of the real photon in terms of its hadronic (long-range) and non-hadronic (point-like) behaviour can be reasonably well extrapolated into the g^2-domain of the virtual photon interaction. In fact the success of the quark-parton model in explaining many features of the hadronic final states in low Q^2 electron and muon scattering and the vector dominance model in explaining photoproduction strongly point towards a single unified explanation of all photon interactions within the framework provided by the quark-parton model together with Quantum Chromodynamics. The ability to carry out experiments at higher energies has in general simplified both the experimental and theoretical understanding.

§1. Total Photon Cross-Sections

1.1. Hydrogen

The measurement of real photon cross-sections has been carried out by a U.C.S.B.-Toronto-F.N.A.L. (U.T.F.) group[2] in a high precision experiment (systematic error ~0.7%) using tagged photons up to an energy of 185 GeV. The main source of difficulty in achieving such precision is caused by the electromagnetic pairs whose cross-section is ~200 greater than the hadronic cross-section. The photon energy range has been extended down to 18 GeV to provide a comparison with lower energy data.[3] The results, illustrated in Fig. 1, show that the photon behaves very much like a hadron in that the cross-section has a broad minimum around a photon energy of 40 GeV and rises by ~4 */ub* over the measured energy range. A straight line fit to the data for $E_r > 35$ GeV gives:

$$a_r(rp) = -(112.76 \pm 0.41) + (0.0272 \pm 0.00050) E_r \quad \wedge$$

which is very similar to that obtained in hadron-induced total cross-sections. This comparison can be made qualitative using vector dominance which relates

$$\sigma_T(\gamma p) = \alpha \sum_V (4\pi/\gamma_V^2)\sigma_T(Vp)$$

and the quark model which relates *o(Vp)* to the measured hadronic cross-sections. The curves given in Fig. 1 show that if the energy dependences of all the *p,* o> and *(j>* cross-sections are representative of all the components of a_r for the higher vector mesons then it is difficult to fit the data. It has been suggested by the U.T.F. group that this excess of 2-6 */ub* cross-section could be due to the charm cross-section. This assumption relies heavily on the normalization to the previous lower energy data and it is doubtful to use the Vector Dominance Model to explain small differences at the 5 % level.

1.2. Complex nuclei

The U.T.F. group have also measured the total photon cross-section in different nuclei which is of interest mainly due to the concept of shadowing. Shadowing has been observed at lower energies,[4] and is caused by the "hadronic" part of the photon being absorbed by nucléons on the front surface of the nucleus. The main interest in going to higher energies is to measure the amount of shadowing since there have been conflicting results as to the amount at lower energies.[5] In addition, vector dominance arguments can be

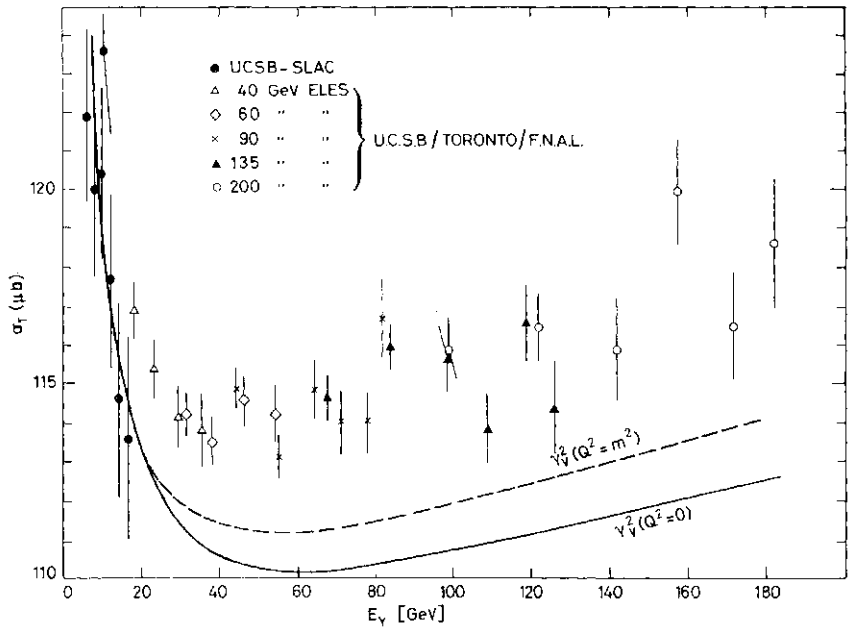

Fig. 1. *o(yp)* total photon cross-section versus E_γ for U.T.F. experiment. Curves are fits to the energy dependence given by *p*, <*o* and *(f>* cross-sections using *y — V* couplings given by photons ($Q^2=0$) and e^+e^- ($Q^2 = m_v^2$).

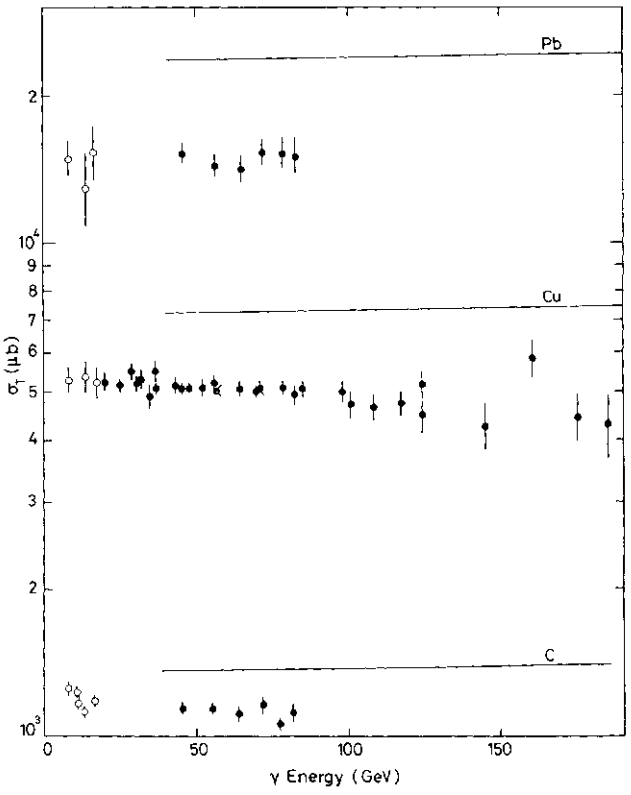

Fig. 2. *G(JA)* total cross-section versus E_γ for C, Cu and Pb targets. The solid lines are *A* times the energy-dependent fit to the H_2 data. $, U.C.S.B.; +, U.T.F.

used to show that higher mass vector mesons should increase the amount of shadowing since the distance travelled by the meson in the nucleus ~*2E/Mv*-

The results are presented in Fig. 2 for Carbon, Copper and Lead, where the solid line is A times the energy dependent fit from H_2 for $E_\gamma<35$ GeV, *i.e.*, neglecting small effects due to proton-neutron differences. There is clear evidence for shadowing, and the results on Copper are in good agreement with the lower energy data of the previous measurements of the U.C.S.B. group at SLAC.[6] There is little energy dependence of the Copper data by itself, but in order to show the effect of shadowing it is simpler to compare the nuclear cross-section with that for free nucléons in terms of the effective nucléon number defined as

$$\frac{A_{\text{eff}}}{A} = \frac{\sigma(\gamma A)}{Z\sigma(\gamma p)+(A-Z)\sigma(\gamma n)}$$

This quantity is plotted in Fig. 3, and shows that there is indeed increased shadowing with photon energy. When more complete data are available, it will be useful to study the behaviour of the cross-section on different nuclei around the region of the broad minimum around 50 GeV in order to obtain a better understanding of the shadowing process. In this region the real part of the scattering amplitude off a single nucléon presumably goes through zero, which will minimise many of the corrections brought about by the real part.

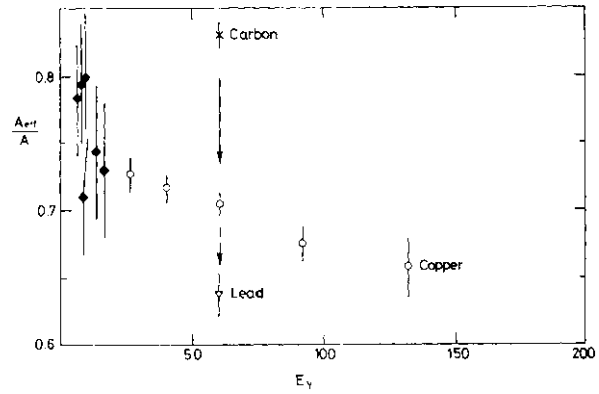

Fig. 3. *Aeft/A* versus E_γ for U.T.F. experiment on different targets. |, U.C.S.B. (Cu); +, Cornell (Cu).

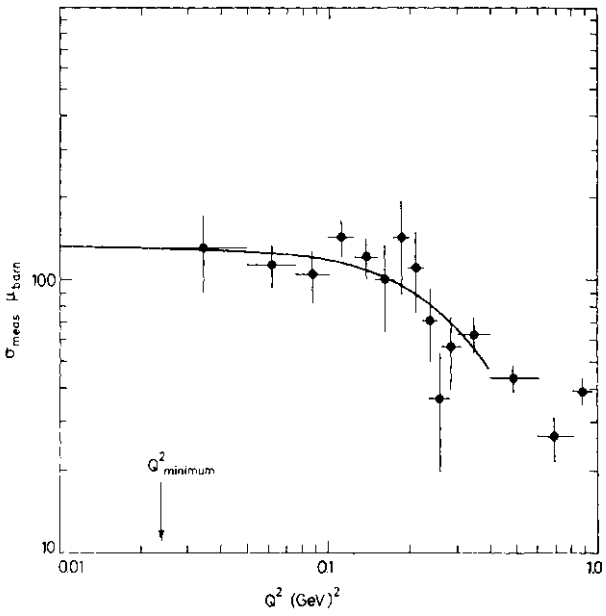

Fig. 4. The total inelastic cross-section on H_2 versus Q^2 in the ν range 170-200 GeV using data from C.H.I.O. Fit given in text.

§2. Inelastic Structure Functions Including Determination of *R*

2.1. Comments on R

The study of inelastic lepton scattering enables the photon to be taken off the mass shell and introduces two cross-sections for longitudinal and transverse photons whose ratio R is related to the structure functions W_1 and W_2 or F_1 and F_2. The Q^2 dependence of the inelastic cross-section has been measured by the Chicago-Harvard-Illinois-Oxford (CHIO) collaboration[7] at very small Q^2 in the energy range 170-200 GeV and the results are presented in Fig. 4. A fit has been made to the data of the form

$$o_{me}UQ^2)=\wedge UQ^2\text{-}0)[A^2l(q^2+A^2)]$$

giving

$$A=0.09\pm0.03 \text{ GeV}.$$

In order to relate this cross-section to photoproduction it is necessary to know i?, since $R=0$ gives $\wedge_r=132\pm13$ */ub* and $R=0.5$ gives $<7y=113\pm13$ *fib.*

The importance of R can also be understood in terms of the quark-parton model where R, which is a function of $x=Q^2/2Mv$ can be written as

$$R(x)_{\text{prim}}=\sigma_L/\sigma_T=4(M_Q^2+p_\perp^2)/Q^2$$
$$=4p_\perp^2/Q^2 \text{ (Quark mass}=0)$$

where $p_\perp$ is the transverse momentum ol the valence quark inside the nucléon and is now known from Drell-Yan type measurements to be as large as ~800 MeV/c. In addition to the primordial contribution (related only to the target nucléon at rest) there is an additional contribution from the dynamics of the intereaction which is given by Q.C.D. and is a slowly varying function of Q^2. For reasons of simplicity, since both contributions are related, R can be expressed as

$$R(x)=R(x)_{\text{prim}}+R(x)_{\text{dyn}}$$
$$=4p_\perp^2/Q^2+1/\log(Q^2/\Lambda^2).$$

The most precise range of data on R comes from the different SLAC experiments and the results of this compilation presented at the Conference[8] are presented in Fig. 5, where the values of R obtained for each Q^2 and W^2 region have been derived from a large set of kinematic data points which are all very consistent. There is no obvious strong dependence on Q^2 or W^2 and the average value of R is $<i?)_{wt.ave}=0.21\pm0.1$ which is somewhat smaller than that given a year ago of 0.25zh 0.1.[9]

In order to study the dependence of R on x, this has been plotted in Fig. 6 for different values of Q^2, together with the theoretical Q.C.D. predictions.[10] The data are in good agreement at low Q^2, but generally lie above the theoretical predictions for larger Q^2. It is clearly important, but difficult to measure, to have more precise data on R as a function of x and Q^2, since the quantity is related to the transverse momentum of the quarks within the nucléon. A determination of R from neutrino experiments in the range $q^2>\backslash$ GeV^2 gives smaller values.[11] However, the uncer-

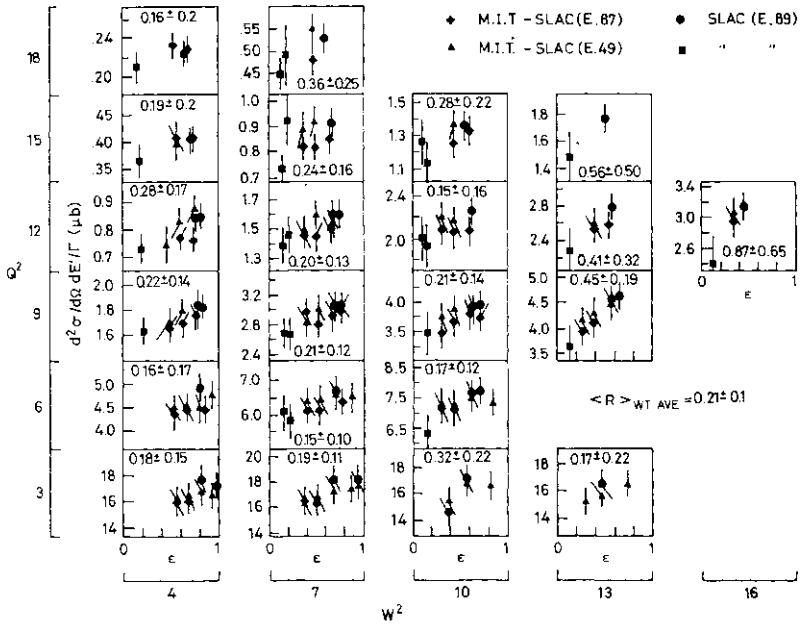

Fig. 5. Value of R obtained from measurements at each value of g^2 and W from SLAC-MIT data.

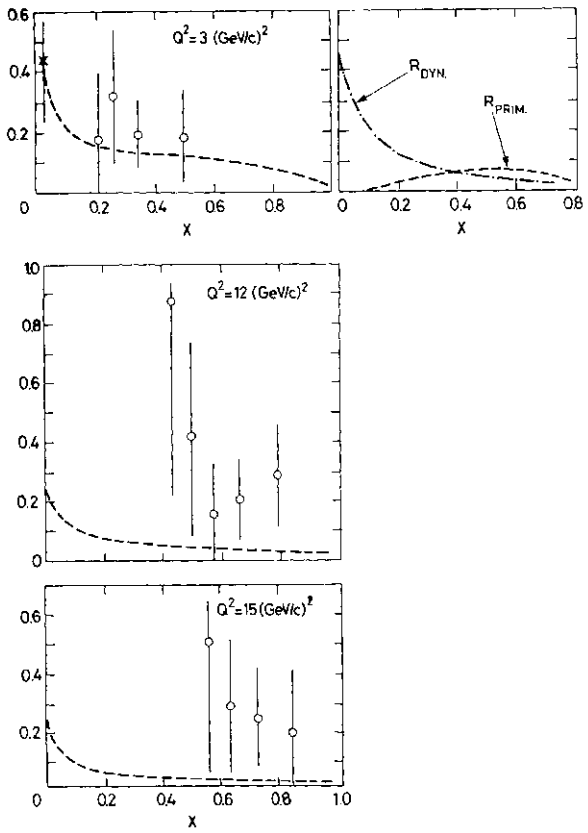

Fig. 6. The variation of R with x at fixed Q^2. The dotted curve is the Q.C.D. prediction. ⊕, SLAC-MIT; C.H.I.O.

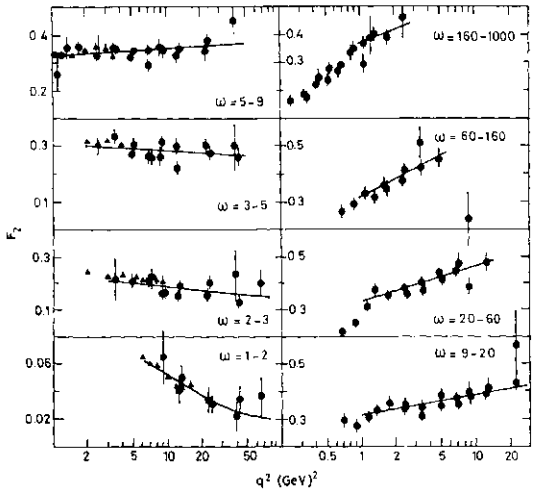

Fig. 7. Variation of F_2 with Q^2 for different ω regions. +, C.H.I.O.; I, SLAC. Solid line is fit given in text.

tainty in R does not have much effect on the determination of νW_2, as will be seen below.

2.2. νW_2 structure function from H_2

The most recent data on the structure function νW_2 (or F_2) have been obtained by the CHIO Collaboration[12] and extend their previous H_2 measurements down to smaller x (larger $\omega = 1/x$) values, using 219 GeV muons. The q^2 dependence of the structure function νW_2 is plotted in Fig. 7 together with the older SLAC data and shows the familiar pattern of scaling violations. The indicated errors are statistical and the overall systematic error has been estimated to be 5%. The solid line is a fit to the data using a q^2 power law dependence of the form

$$F_2(x, Q^2) = F_2(x, Q_0^2)[Q^2/Q_0^2]^b$$

where Q_0^2 has been chosen as 3(GeV/c)^2. The value of R used in the extraction of F_2 was

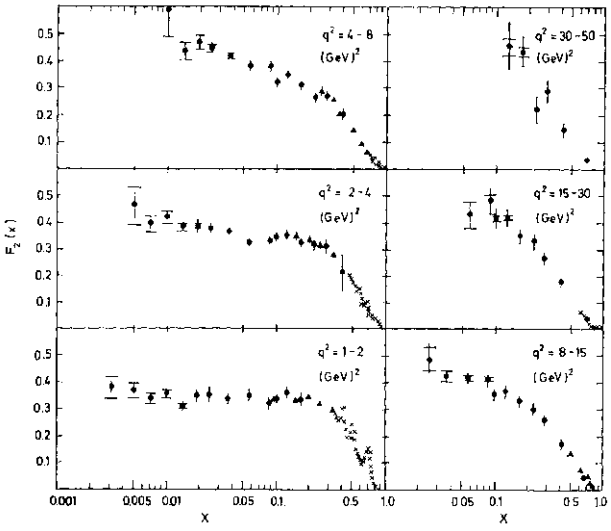

Fig. 8. Variation of F_2 with x for different Q^2. Large horizontal bars indicate a total change in R of 0.5. 4, C.H.I.O.; |, ^ (resonance region), SLAC.

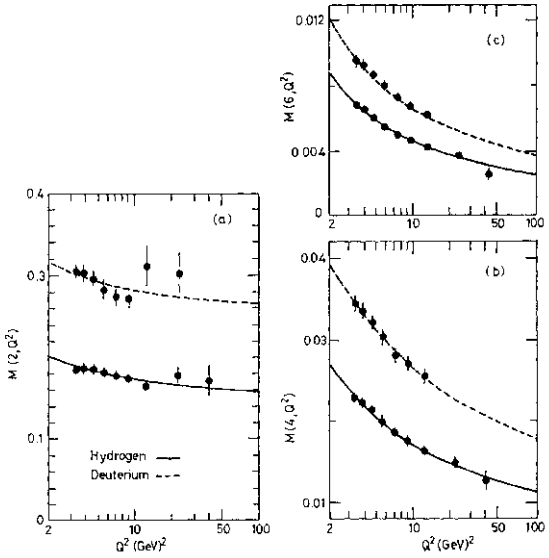

Fig. 9. Nachtmann moments versus Q^2 for H_2 and $Z>_2$ C.H.I.O. data.

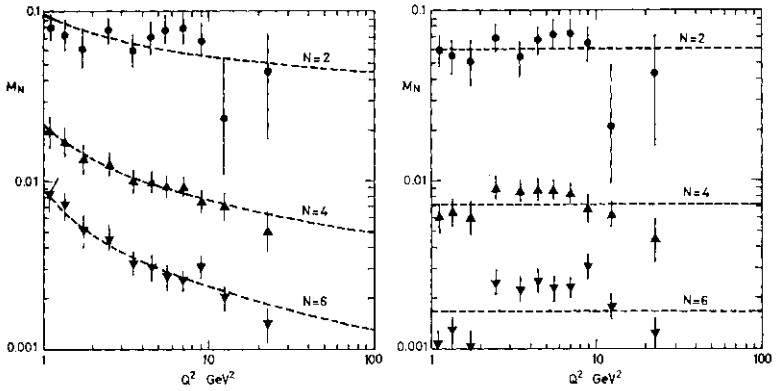

Fig. 10. Moments of $F^{\wedge}$-F_2^N versus Q^2 for C.H.I.O. data and SLAC data. The L.H.S. differs from R.H.S. by the inclusion of the elastic channel.

i?=0.44 based on measurements at 96, 147 and 219 GeV. The change in F_2 due to a change in R can be seen in Fig. 8 where the horizontal upper and lower bars indicate a change in R by ±0.25. This clearly shows that the rise in F_2 with Q^2 at small x cannot be removed by reducing R. It is interesting to note that for fixed Q^2 in the region l-2(GeV/ *cf* there is no evidence of any decrease in F_2 down to the smallest x.

Scaling variations can at present be explained in terms of the theory of Q.C.D., which is an extension of the Quark-Parton model to include gluon emission. In analogy with Q.E.D., it is necessary to measure

$$\alpha_s = \left[\frac{12\pi}{33-2N_{fi}}\right]\frac{1}{\log(Q^2/A^2)}$$

where N_n is the number of flavours. The theory is most rigorously tested through a determination of the ratio of the moments of the structure functions, given by

$$M_i(Q^2) = \int_0^1 dx[x^{n-2}]F_i(x, Q^2)$$

The Nachtmann moments are usually plotted, where x is replaced by the Nachtmann variable $\pounds = 2x/\{1 + Vl + (4M^2x^2IQ^2)\}$," since these take into account mass effects. However, in order to show the comparison with the experimental data, the Nachtmann moments are plotted for H_2 and D_2 data versus Q^2 in Fig. 9 and a value extracted of

$$A = 0.66 \pm 0.08 \text{ GeV}.$$

In general, the moments analyses give a larger value for A than that obtained by fitting the structure function directly. All these analyses involve three terms with different Q^2 varia-

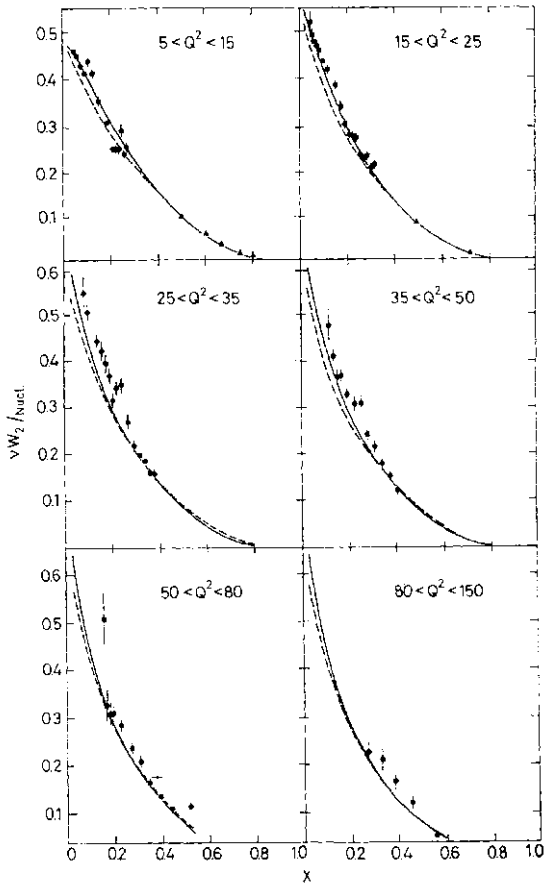

Fig. 11. *v* ^/nucléon versus *x* at fixed Q^2 for M.S.F data (+). The solid and dashed lines are Q.C.D fits, i, SLAC-MIT (Z)ₛ).

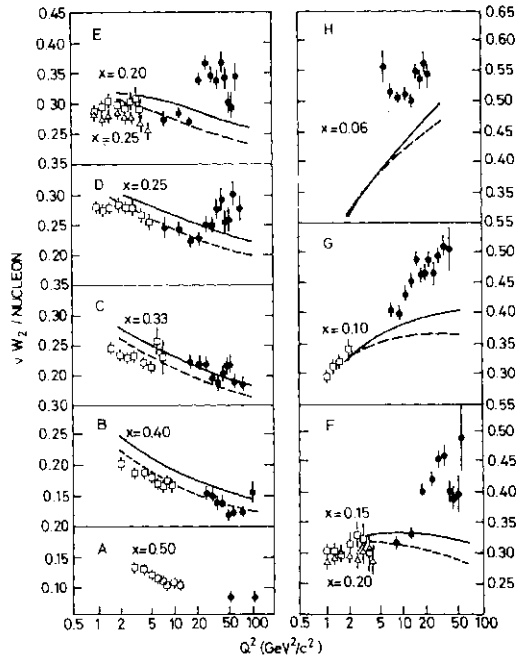

Fig. 12. *v* Jfynucléon versus Q^2 for different *x* ranges. Curves are Q.C.D. predictions. **4,** SLAC-MIT.

tions, whereas an analysis of $Fi \sim\sim F_2$ involves only one term—the flavour non-singlet term. The results of this analysis by the CHIO Collaboration are plotted in Fig. 10, and an excellent fit is achieved using /1=0.675±0.100 GeV. The necessity of including the elastic channels is seen in the fits to the higher moments, which are weighted by the contribution at large *X*. At present all results from deep inelastic scattering from H_2 and D_2 targets are in excellent agreement with the Q.C.D. predictions, but much more precise data will be required to see the effect of higher order corrections.

2.3. Structure functions from complex targets

New high precision data have been reported to this conference by the Michigan State-F.N.A.L. (M.S.F.) collaboration,[14] who have extended their previous measurements on νW_2 up to g^2=150 (GeV/c)² and *W=2*\ GeV. The target consisted of a 7.4 m long iron-scintillator calorimeter (4.260 g/cm²) and recorded 10^6 events (Q^2>5 (GeV/c)² using 3.10^{10} incident muons of 270 GeV. The overall systematic and normalization uncertainties were 10%. Figure 11 shows νW^/nucleon as a function of *x* for different values of Q^2 where the solid *(A=0.5)* and dashed *(A=0A)* are Q.C.D. predictions.[15] The data are in good agreement with the predictions and therefore the existing data in the lower Q^2 range up to Q^2=25 (GeV/c)², but a systematic difference appears at higher Q^2. This difference is seen more clearly in Fig. 12, where the structure functions are plotted versus Q^2 for different values of x_9 and the same Q.C.D. predictions are illustrated. The increase in νW_2 at small *x* and the decrease at large *x* with increasing Q^2 is apparent, together with a strong enhancement in the region of Q^2= 50 (GeV/c)². The possibility of this enhancement having *W* dependence has been studied by the M.S.F. group using the H_2 data from C.H.I.O. and SLAC-MIT experiments. Figure 13a shows all this data plotted in the form *b(x)* against log (1 —*x)* where *b* is given by the power law Q^2 dependence given previously. Figure 13b shows the M.S.F. data for two different ranges of *W* and indicates that the enhancement has a threshold at *W*= 10 GeV.

It is difficult to explain this effect in any obvious way with the *Y* meson, since even

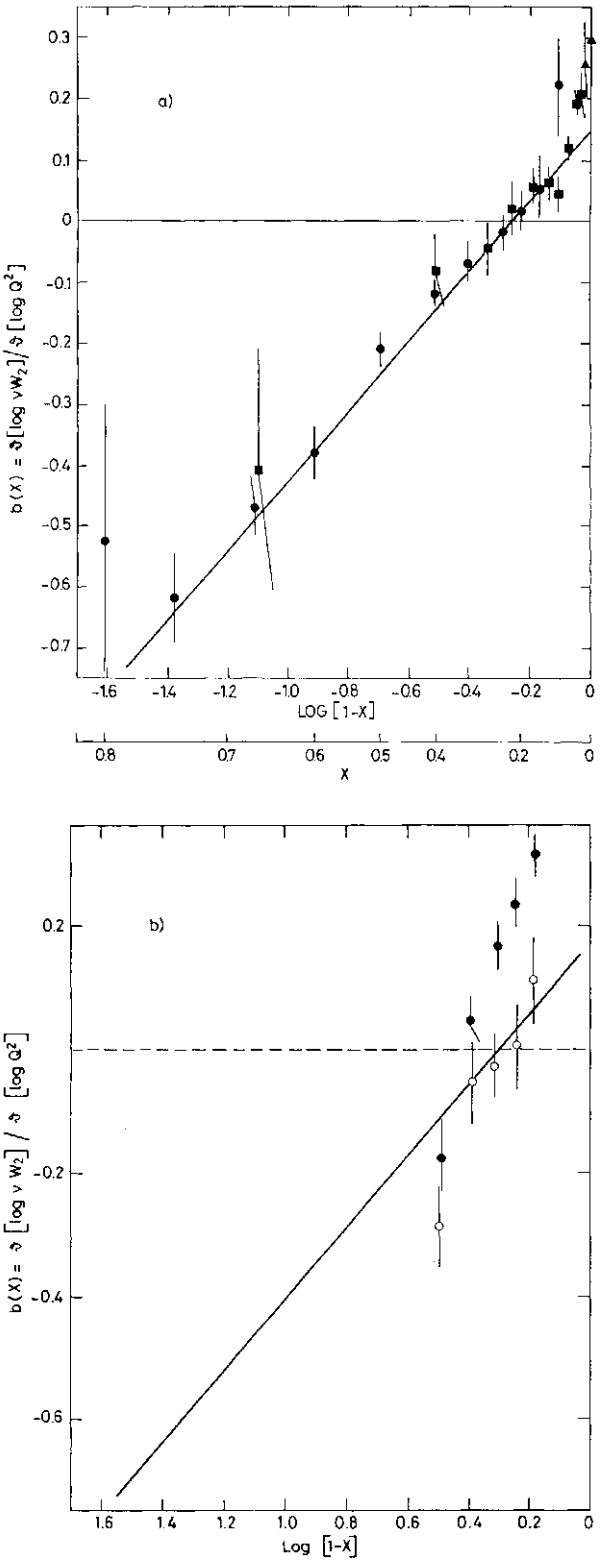

Fig. 13. (a) Slope parameter *b(x)* versus log(1— *x).* Straight line is fit to • CH.I.O. (#²<40 (GeV/*c)²);* + SLAC-MIT(^²<16(GeV/c)²); | CH.I.O. 219 GeV only.
(b) M.S.F. (PF<10GeV); +, M.S.F. (no HP cut). Fit is that given in (a).

allowing for propagator effects, the photoproduction cross-section should be much too small.[16] Results from new experiments at

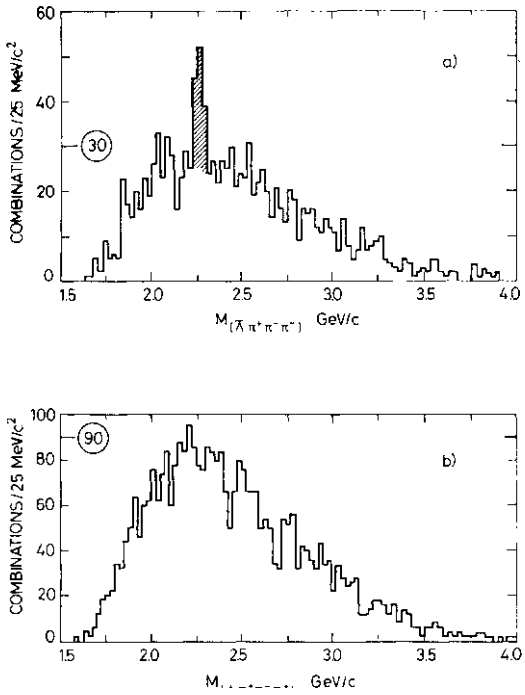

Fig. 14. (a) *Aîr7r~Tc~* mass spectrum,
(b) *A7t~7r7z'* mass spectrum for previous C.I.F. photoproduction experiment.

F.N.A.L.[17] and CERN[18] will be important in verifying these results which violate Q.C.D. predictions, since data from neutrino experiments have not yet attained the necessary precision in this Q^2 range.

§3. Evidence for Charm in Photoproduction

Photoproduction has always been considered as a likely reaction in which to see charmed hadrons. The coupling of the *cc* state to the photon is identical to that of the *uû* state and estimates using different models[19] indicate that the charm cross-section should be ~ 1 % of the total cross-section, *i.e.,* ~ 1 */ub.* Indeed, the first evidence for charm outside *e⁺e~* reactions came from the Columbia-Illinois-FNAL (C.I.F.) Collaboration[20] who found a peak at 2.26 GeV in the *Atc+iz~tz~* anti-baryon mass spectrum but not in the *Atz+tz+tz'* baryon mass spectrum. The results of that experiment are illustrated in Fig. 14. Results from three experiments have been presented to the Conference using photons to search for charm, but so far there are no results on charm or <*p* production using virtual photons where it should be possible to tune the signal to background using the Q^2 dependence of the propagator.

The first experiment has been carried out

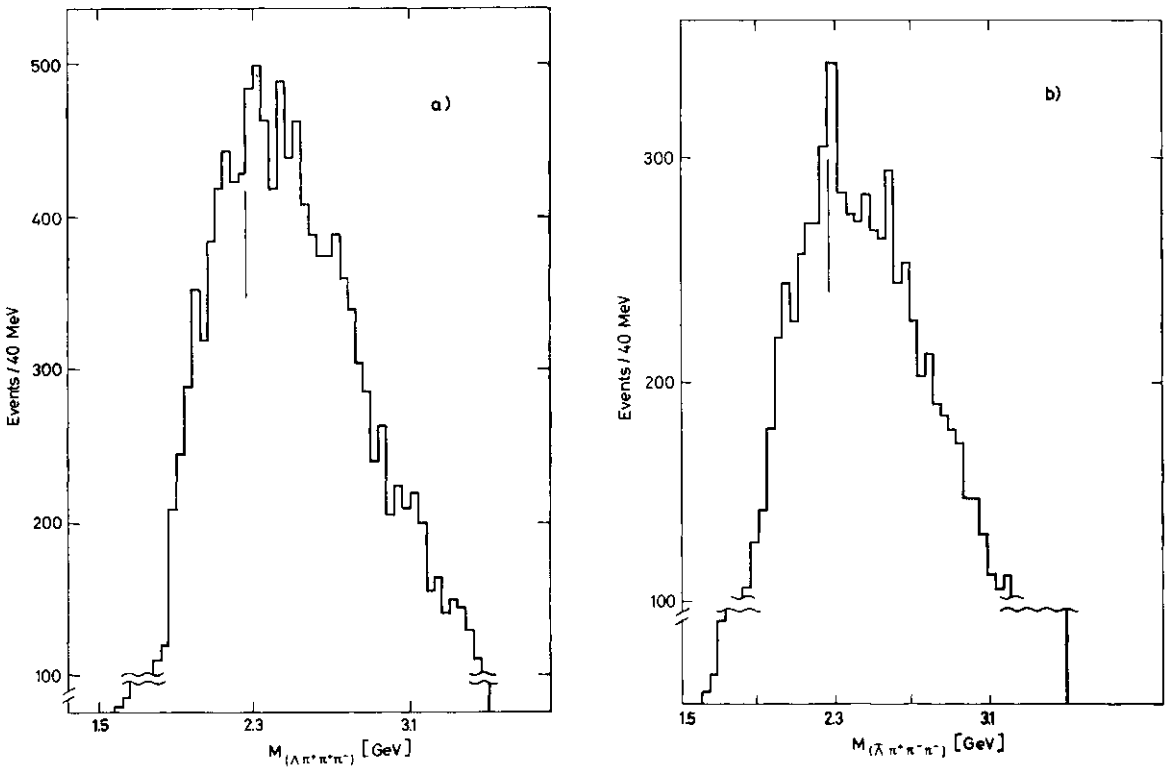

Fig. 15. (a) *An+iz+n'* mass spectrum.
(b) *AIZ~IZ~TZ+* mass spectrum in new C.I.F. experiment. Vertical line occurs at 2.26 GeV.

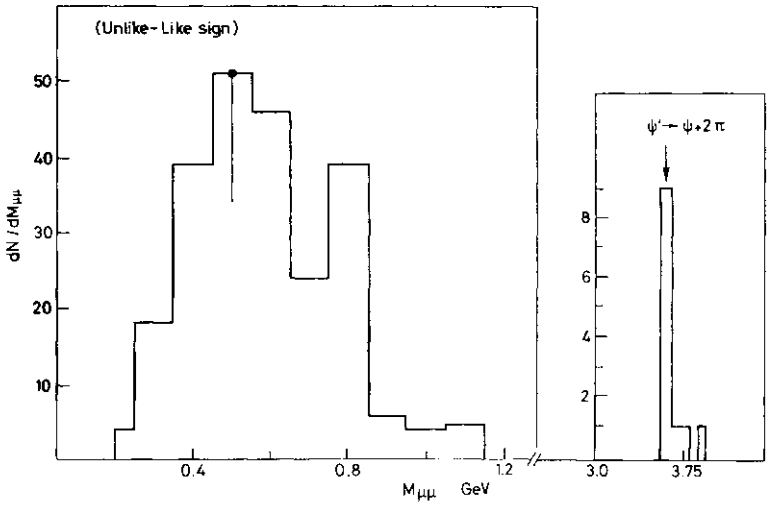

Fig. 16. ***Ni^^—Ni^)*** muon pair mass spectrum in new C.I.F. experiment. Also indicated *<p"-+iz*'n~<p* where *<p-+fj,' pL~.*

by the C.I.F. Collaboration[21] using a wide-band photon beam of maximum energy 300 GeV. The apparatus consisted of a forward magnetic spectrometer containing Cerenkov counters for particle identification, and usd a solid CH target. The sensitivity of the experiment was 200 events/nanob. Preliminary results from this experiment are presented in Figs. 15aandbforthe *ATZ+TI+TZ-* and *AK+'K~TI~* mass spectra. The peak is again visible at 2.26 GeV, but there is some evidence of structure in the neighbourhood of the 2.26 GeV region in the mass spectra. Special runs have been performed to study the effects of ^-induced reactions, since these are contained in the broad band beam. Preliminary results also show structure in the region around 2.26 GeV,[22] and further detailed analyses of these backgrounds are under way.

A search has been made by the same group for *DD* production through the *JU'JU~* pair mass spectrum by the decay *D-^fx^X* (~ 10%).

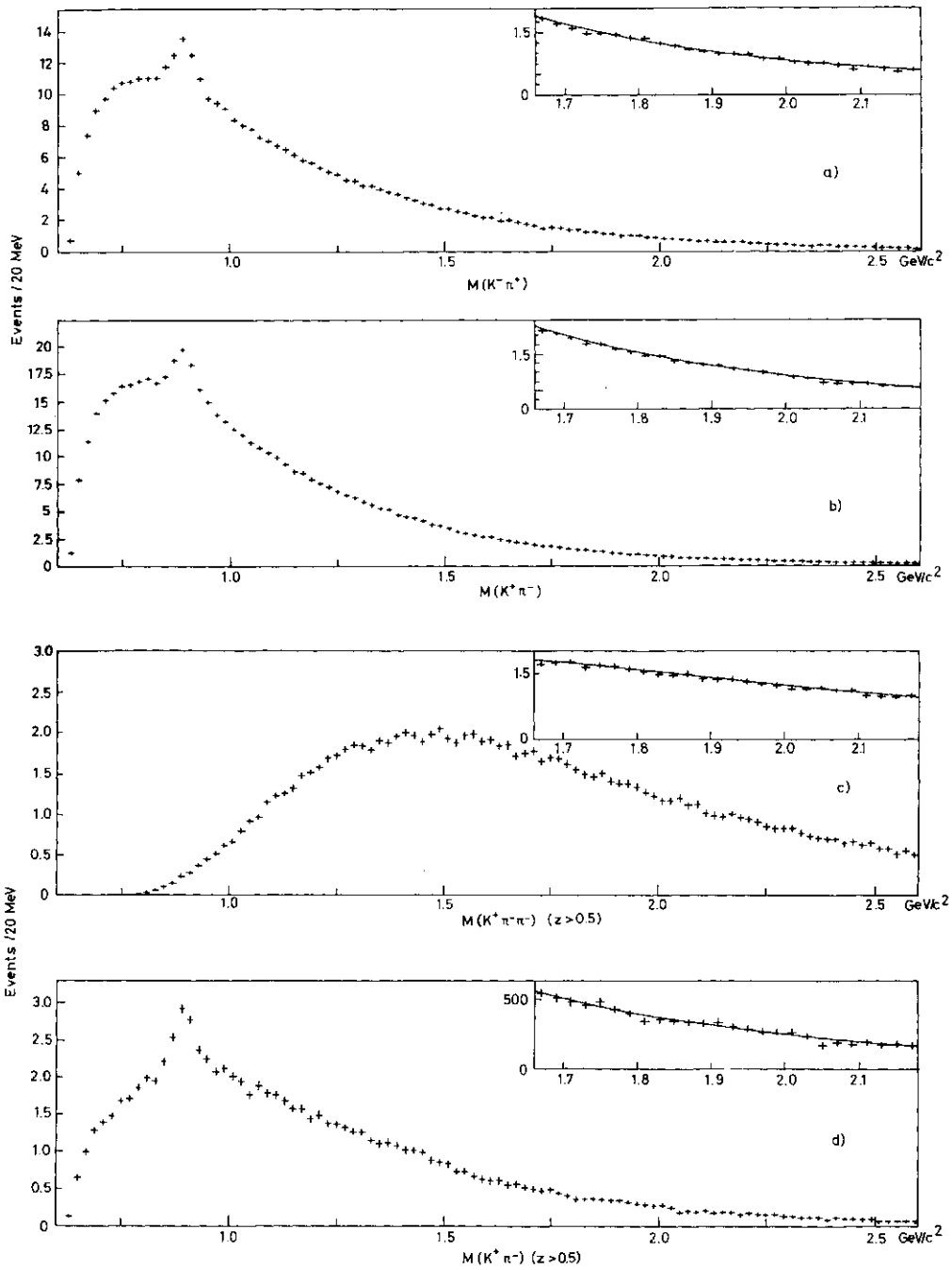

Fig. 17. (a) *K~7r* mass spectrum.
(b) *K7r~* mass spectrum.
(c) *K7T~TC~* mass spectrum (z>0.5).
(d) *K n~* mass spectrum in WA4 CERN-Omega experiment.

The lepton spectrum from *D* decay at rest is known to peak around 300-400 MeV/c, therefore the mass spectrum for *N(/u /u~)—N(/bi)* should show an enhancement in the low mass region if all backgrounds are properly taken into account. Figure 16 contains the results of the resulting subtracted muon-pair spectrum and there is an enhancement in this preliminary data at low mass. However, it will be necessary to determine the production of *p, o)-±fi fi~* (including the mass region below the *p°)* and possible Dalitz decays of the *w* and *r]* mesons into muon pairs in order to determine the shape of the background mass spectrum. Also indicated in Fig. 16 is the mass spectrum of the *<p'->(ju JU~)+7T7U~* where the muon pairs in the *<p* mass region were assumed to have the *<p* mass. This is the first indication of *<p'* production in photoproduction and underlines the analysis power of the spectrometer.

The second experiment has been made by

Table I. Properties of trident-like events

Event	Decay path (μ)	E_γ	Tracks charge/momentum (GeV/c)	Angular aperture (deg)	Invariant mass (GeV/c^2)	Decay time (sec)
(a)	16±4	64.1	1) +23.913 } E_{vis} 2) + 7.759 } 39.6 3) − 7.899	3.4±0.2	π π ~1.1 ±.2 π	0.2 10^{-14}
(b)	30±2	65.1	1) +37.452 } 38.3 2) − 0.800 } 3) − 0.100 : 0.500	6±0.2	K π ~1.2 e	0.46 10^{-14}

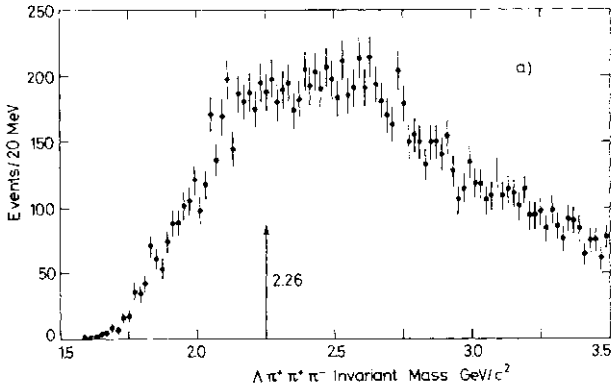

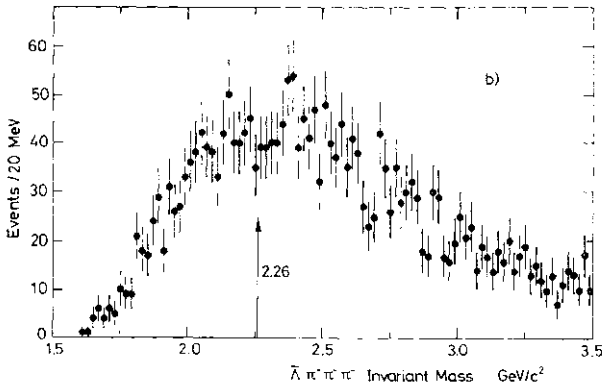

Fig. 18._ (a) *Aiz7i~7z~* mass spectrum.
(b) *An-iz+Tz** mass spectrum in WA4 CERN-Omega experiment.

the WA4 CERN-Omega Collaboration[23] using the large multi-particle spectrometer in conjunction with a H_2 target. The incident beam was tagged in the energy interval between 20 and 70 GeV and the experiment had a sensitivity of 60 events/nanob. The results of this experiment are illustrated in Fig. 17 (a-d) for the *K^ic^it*)* mass spectrum expected from *DD* meson decays. There is no evidence of any peak in the *D* meson mass region, even after demanding that the *D* mesons have large longitudinal momenta. This highlights one of the major difficulties in all these experiments where multi-combinatorial backgrounds arise from the strange-particle cross-section, which is at least ten times that of the charm-particle cross-section and where the *D->KTZ* is ~ 1 %.

Table II. Summary of results from three charm experiments.

Experiment	Channel	Comment	σ_c
COL/ILL/ FNAL	$\bar{\Lambda}$ 3π	Peak at same mass	0.1–1 μb
	$K\pi$, $K2\pi$	Not seen	
	$\mu^+\mu^-$	Not proven	
CERN SPS (Ω) WA4	$K\pi$, $K3\pi$	Not seen	≤0.5 μb
	3π, 3π	Not seen	Model dependent
EMULSION GP+WA4	2 *D* events seen		≥0.5 μb

The WA4 Collaboration have also studied the *A7t'K'n~* and *ATZ'TZ'TZ^* mass spectrum where a forward kaon or proton was demanded in the trigger. The results are plotted in Figs. 18a and b, and no enhancement is visible in the region of 2.26 GeV.

The third experiment has been performed by an emulsion group in association with the WA4 Collaboration,[24] using the CERN-Omega spectrometer and nuclear emulsions as targets. The group have been able to locate 482 hadronic vertices in the emulsion and from these events two candidates have been found which satisfy their criterion of short-lived trident-type events. Their properties are listed in Table I.

The life-time of these two candidates is very short compared with the theoretical predictions of 6x 10~[13]s,[25] but if accepted as charm candidates, then a lower limit can be set of 0.5 ***/ub*** for the charm cross-section at the 90% confidence level, when all the correction factors and efficiencies are included.

Table II is an attempt to summarise the results of all three preliminary experiments from which the following conclusions can be drawn:

a) Charm particle production should be seen at the level of ~0.5 ***/ib.***

b) The production of a charmed anti-baryon is seen, but it is difficult to understand

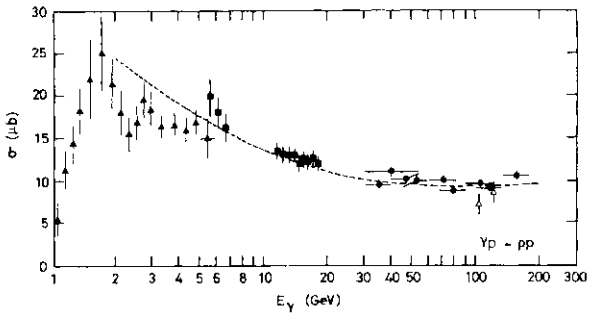

Fig. 19. *oijp^p^p)* versus *E,.* The dotted curve is fit to V.M.D. relationship using hadronic o_T values. +, DESY; +, SLAC; U.T.F.; **4,** C.H.LO.

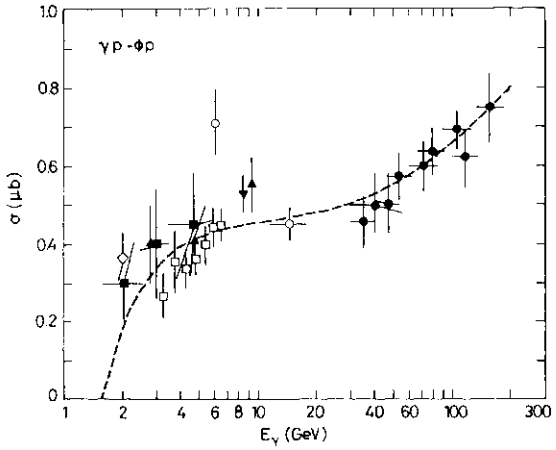

Fig. 20. *<j{jp-^<i>p)* versus E_γ. The dotted curve is a fit to V.M.D. relationship using hadronic a_T vaules. DESY; !,LBL/SLAC; **f**, BONN; SLAC; ±. U.T.F.

why there is no charmed baryon signal. The fact that no signal is seen at lower energies suggests a strong energy dependence which is not apparent in photoproduction of *pp* pairs. The possibility of ^-induced production has to be resolved.

§4. Vector Mesons of Mass <3 GeV

4.1. Production of p, co, § mesons by real photons

The reaction *j+p-^p°+p* has been measured at high energies by the U.T.F. Collaboration[26] using a tagged photon beam in the energy range up to 200 GeV. The energy dependence of the cross-section is plotted in Fig. 19 where the dotted curve is obtained from the relationship given by (V.M.D. + Additive Quark Model):

$$\sigma(\gamma p\to\rho^0 p) = (\alpha\pi/\gamma_\rho^2)\tfrac{1}{2}[\sigma(\pi^+ p\to\pi^+ p)+\sigma(\pi^- p\to\pi^- p)]$$

using experimental data from pion elastic scattering measurements[27] and $7^{*2}/4\mathbf{tt}=0.64$, which is the value extracted from *p°* studies in complex targets. Clearly at higher energies *<j(jp-*P°p)* would be expected to show the same increase with energy as that seen in pion total cross-sections and *o,{jp).* No new results have been presented in *to*[0] photoproduction.

The reaction *j+p-+<f>+p* is of interest since it cannot have any meson or baryon exchange in the *s* and *t* channels through the OZI rules[28] and therefore this reaction has a high-energy Pomeron-type behaviour from very low energy (~ 2 GeV). Three results have been presented to this conference covering three widely different energy regions.

A high-precision experiment has been performed by a Daresbury-Lancaster-Sheffield Collaboration[29] in the photon energy range 3-5 GeV, extending the '/'-range out to 1.3 $(GeV/c)^2$. The results show that there is a distinct break in the /-slope around /=0.4 $(GeV/c)^2$ and are consistent with ^-channel helicity conservation throughout the entire *t*-range. Results have been presented by the WA4 CERN-Omega Collaboration[30] in the energy range 20-35 GeV which are consistent with a constant cross-section. Finally high-energy measurements have been performed by the U.T.F. group[31] in the photon energy range up to 150 GeV. The results are shown in Fig. 20 and again give very beautiful evidence of the success of (V.D.M.+Additive Quark Model) using the relationship linking the *yI/4TI:* with the measured values of the K^+, *K~* and *TC~* total cross-sections. The spectacular increase in the total cross-section comes from the fall and rise in the *K~p* cross-section superimposed on the continually rising K^+p cross-section. Similar effects should be present in the *<fi* total cross-sectional behaviour at high energies which could be used to shed light on the behaviour of *Dp* total cross-sections.

4.2. Production of p, a),, <j) mesons by virtual photons

The production of *p, co* and *<p* mesons by virtual photons requires the separation of longitudinal and transverse cross-sections in order to compare with the V.D.M. model which predicts that the transverse cross-section should fall like the square of the propagator term

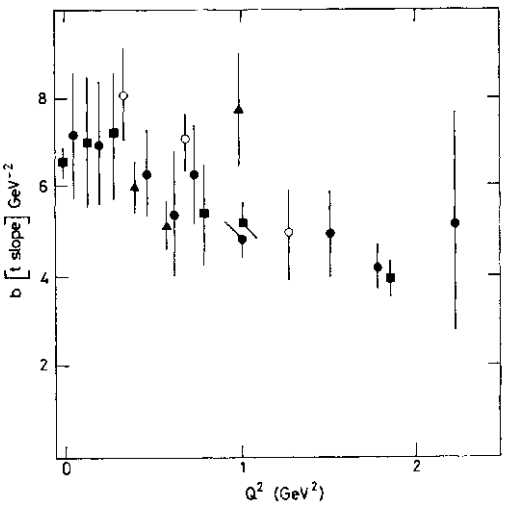

Fig. 21. The slope parameter b for $\gamma_V + p \to \rho^0 + p$ as a function of Q^2. ♦, Cornell $\langle W \rangle = 2.5$ GeV; ♦, Cornell $\langle W \rangle = 3.2$ GeV; ◊, UCSC/SLAC; ♦, SLAC.

$m_V^2/[Q^2 + M_V^2]$.

i he results of experiments on *p''* production, where the broad skewed ττ+ττ' mass spectrum makes separations difficult to perform, are in reasonable agreement with this picture. Results presented to this Conference from the Cornell group[32] and the SLAC-U.S.S.C group[33] however indicate that in general the data points lie below the V.D.M. predictions in the Q^2 range up to 2.5 (GeV/c)^2 and $2 < W < 5$ GeV. Results from the same two groups on *o)°* production indicate that the ratio ***a^j (TpO*** is constant in the same Q^2 and Grange.

An interesting question, first raised at the 1971 Electron Photon Conference[34] was the possibility that the radius of the photon would shrink with Q^2. This would manifest itself *via* the optical model in a decrease of *b* with g², where è, the slope parameter, measures the radius of the interaction and reflects the combined size of the photon and proton. An experiment has been carried out by the Cornell group[35] and the results are sufficiently precise to show that *b* does decrease with Q^2 as illustrated in Fig. 21. However, published data exist on ç5 electro-production measurements[36] which show no evidence of shrinkage. Further experiments are required at high energy in order to resolve this question completely.

43. Higher mass mesons beyond p, œ and <f>

The search for higher mass vector mesons in the region between 1 and 3 GeV is important to look for new vector mesons containing

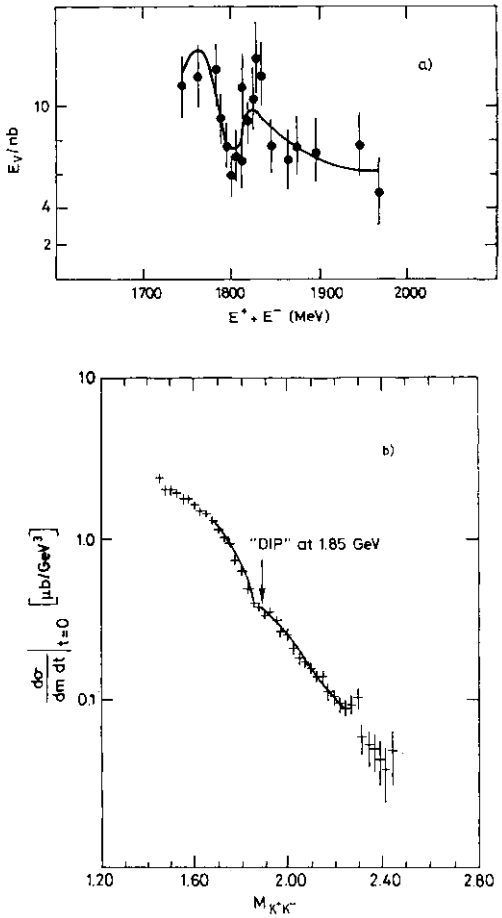

Fig. 22. (a) Cross-section *(n>3* charged tracks) for *BB* group (Frascati).
(b) The photoproduction cross-section versus *K'K~* pair mass in Cornell-Harvard experiment.

(w, *d, X)* quarks, multiquark states etc, since there are many confusing results in this mass range both from photoproduction and *e⁺e~* storage rings.[37] The *p'* ~ (1260 MeV) has been obtained from fitting interference spectrum in the process *y'rp->e⁺e~'rp* by a DESY-Frascati-Pisa group,[38] but this state has not been established elsewhere. The *p''* (1500-1600 MeV) has been seen as a broad 300 MeV resonance in 7r'7r~7r'7r~ mass spectrum, and also determined in the *TC'K~* final state from a phase-shift analysis in the reaction *K~p->*

A study has been made of the reaction *yp-*K+ +K~ +p* (assumed) by a Cornell group[39] using a spectrometer to select the two charged kaons. The investigation concentrated on the region around 1800 MeV where various dip structures have been observed in the Frascati storage ring measurements.[40] The results of one of these measurements is indicated in Fig. 22a giving the cross-section as a func-

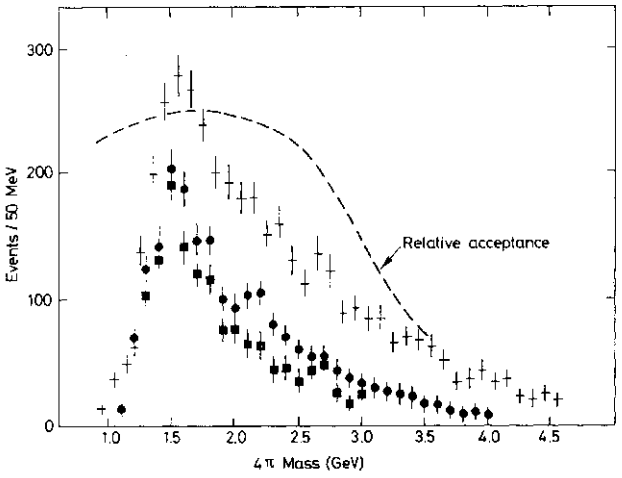

Fig. 23. The $T:^{+}n\sim n^{+}n\sim$ mass spctrum in WA4 CERN-Omega experiment + all / values; + $0</<$ 0.3 GeV^{2}; fritting A $^{+}$ ^ ~ in 1~ state.

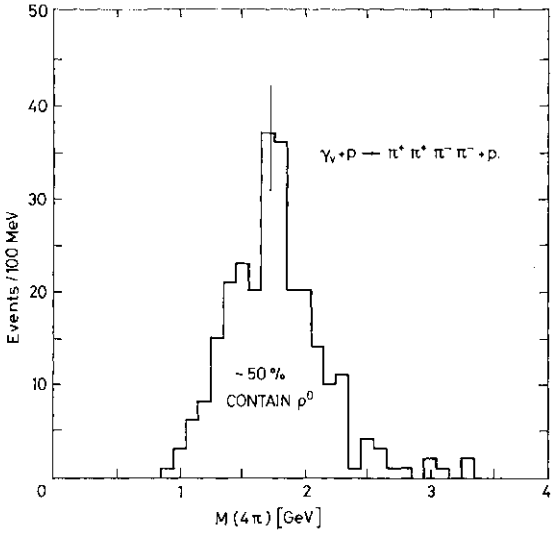

Fig. 24. The $7tK\sim7t\%\sim$ mass spectrum in the Cornell electroproduction experiment.

tion of beam energy into >3 charged particles. The experimental technique was checked using pion pairs where $p°$, $f°$ and $g°$ signals were established and the resulting $K^{+}K\sim$ invariant mass plot is shown in Fig. 22b, where a pronounced dip is seen at a mass of 1.8 GeV. A mass of 1.83^0.013 GeV and a width F=^111 ±23 MeV are determined for this resonance by fitting the mass spectrum with a combination of resonance, coherent and incoherent background. However the parameters obtained for this resoance are sensitive to the phase and form of the background.

The WA4 CERN-Omega Collaboration[41] have studied the reaction $y+p-\wedge n+Tt'Tt+Tc'+p$ and have observed a broad enhancement in the region of 1.5 GeV with a F.W.H.M. of 0.5 GeV as seen in Fig. 23. An investigation of the sub-structure of the 4-pion spectrum shows a very strong $p°$ signal, and the $K^{+}TJ:\sim$ opposite to the $p°$ region has the features of a broad threshold enhancement peaking around 0.5 GeV. A spin-parity analysis indicates that the p'' decays predominantly into $p^{0}7c^{+}n\sim$ with $J^{p}=l\sim$, but there is a lot of structure in the higher mass region. Preliminary results from the electroproduction experiment at Cornell[42] in the range $Q^{2}>0J$ GeV^{2}, $W>2$ GeV show a broad enhancement peaking in the region of 1.8 GeV as illustrated in Fig. 24. Again 50% of the $x^{+}7r\sim$ events occur in the $p°$ region.

The WA4 CERN-Omega Collaboration[43] have also studied the reaction $f+p-*$ $K^{+}K\sim7z^{+}7t\sim p$. The resulting mass spectrum

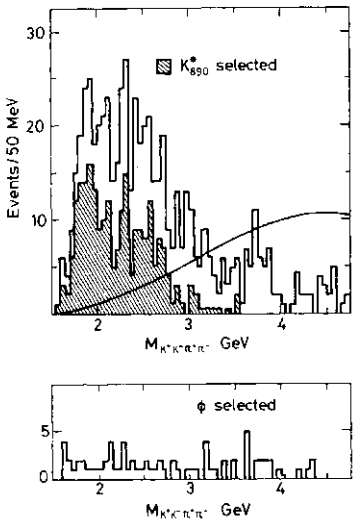

Fig. 25. The $K+K\sim7t^{+}7t\sim$ mass spectrum in the WA4 CERN-Omega experiment. The solid line is predicted mass spectrum for peripheral $K*K\%p$ production.

illustrated in Fig. 25 shows a broad threshold enhancement which has strong $K*$ (890 MeV) and <f> signals in the $K\wedge it*$ and $K^{+}K\sim$ states respectively. There is no evidence for any enhancement in the $\wedge>TZ\wedge TZ\sim$ mass spectrum, predominantly in $K*Kn$. Figure 26 shows the excellent agreement between the $K*K\sim'n*$ mass spectrum measured in the electroproduction Cornell experiment and that from photoproduction.

These broad enhancements in the $pPit+K''$ and $K*K+TZ\sim\sim$ channels are similar in that the decay is predominantly $V*-+V+K^{+}T:\sim\{K^{+}TC\sim)$ where the two pseudoscalar mesons are presumably an .y-wave enhancement. This is

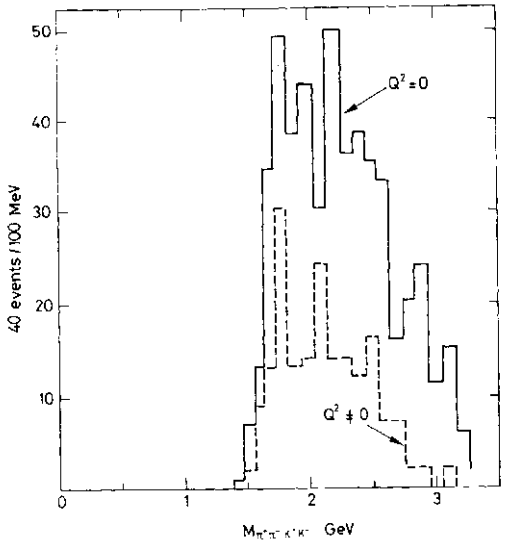

Fig. 26. The $K^{+}K^{-}n^{+}\pi\pi$ mass spectrum in the photoproduction ($Q^2=0$) and electroproduction ($Q^2 \neq 0$) experiments.

similar to what is seen in the decay of $\eta' \to \pi^+\pi^-\eta$ (s-wave).

In the higher mass region >2 GeV, there are indications in data from photoproduction and electroproduction by the previous groups for threshold enhancements in *pp* mass spectra. It is not possible to draw any conclusions on possible baryonium states at this time due to the small number of events. There is a need for much more detailed work to untangle the whole mass region between 1 and 3 GeV, which is clearly rich in spectroscopy but requires special techniques, *e.g.*, polarised photons, decay channels etc., in order to isolate states of different quantum numbers.

§5. Inclusive Final States Involving Hadrons

The inclusive final states involving hadrons in inelastic lepton scattering have been used to test ideas on the simple quark parton model. In general, the inclusive hadron distributions behave very much like those produced from incident hadrons in terms of multiplicity, $x_F = 2p^*/\sqrt{s}$ and p_L distributions. There are certain areas where the deep inelastic process can be used to advantage to simplify the reaction process using the following assumptions (quark-parton model):

(1) Photon interacts only with one valence quark of fractional momentum x

(2) Struck quark with fractional momentum $z=Eh/\nu$ decays into hadron

(3) Factorisation of two processes enabling

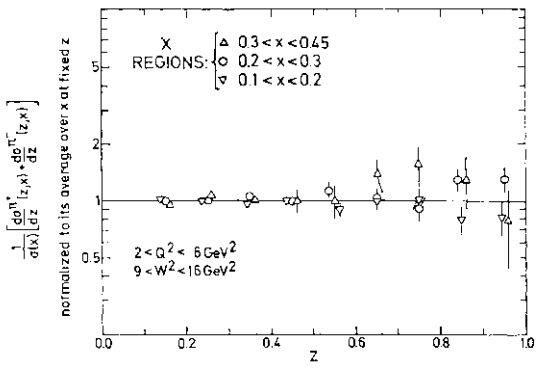

Fig. 27. The sum of π^+ and π^- cross-sections plotted versus z for different x regions in the DESY-Cornell experiment.

determination of fragmentation function $D_u^h(z)$

An experiment has been carried out by a Cornell-DESY group[44] using a streamer chamber and has provided a determination of the fragmentation function for $\pi^+ + \pi^-$, since the contribution due to protons and kaons has been excluded. The data from this experiment ($W^2 \wedge 20$ GeV^2) has been compared with data from the C.H.I.O. Collaboration ($J^{\wedge 2} \wedge 150$ GeV^2), and shows no evidence for W dependence in the quantity

$$\frac{1}{\sigma_{\text{tot}}}\left\{\frac{d\sigma^{\pi^+}}{dz}(x,z)+\frac{d\sigma^{\pi^-}}{dz}(x,z)\right\} = D_u^{\pi^+}(z)+D_u^{\pi^-}(z)$$

which is independent of x due to îsospm invariance and charge conjugation (neglecting strange quarks). There is no evidence of any W dependence to within 20%. Figure 27 gives the above invariant cross-section versus z for different x regions and indicates that the factorisation works reasonably well.

The results of this experiment are compared with those of other experiments in Fig. 28, and show that the agreement is very good as expected from the quark-parton model. The comparison of e^+e^- hadron distributions with those from deep inelastic scattering is clearly seen in the data and is an indication that target effects have to be considered more carefully. The comarison with predictions of different jet models[45] for hadronic production is also included. The separation of the $D^{K^+}_U$ and D^{K^-} has been made using the quark parametrisation of Feynman and Field, and the results are illustrated in Fig. 29 together with the results of neutrino experiments. The

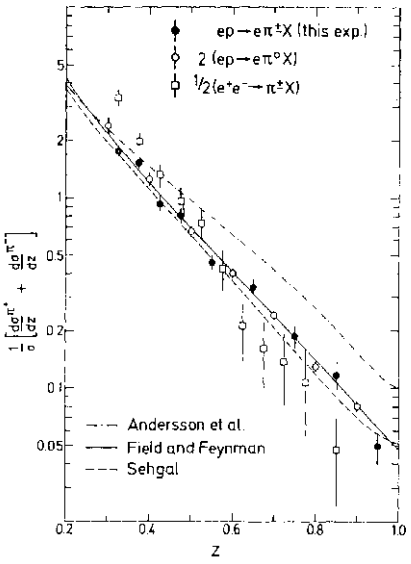

Fig. 28. The sum of n^{+} and $n\sim$ cross-sections plotted against z for Cornell-DESY electroproduction experiment § Aachen-DESY electroproduction experiment and § DASP $e^{+}e\sim$ experiment.

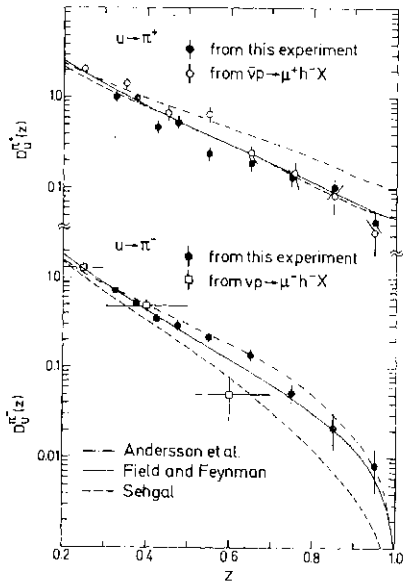

Fig. 29. Fragmentation functions for *u* quark into **T T** ⁺ and *7t~* from Cornell-DESY experiment (+). Also indicated are those for neutrino (^) and anti-neutrino C6\

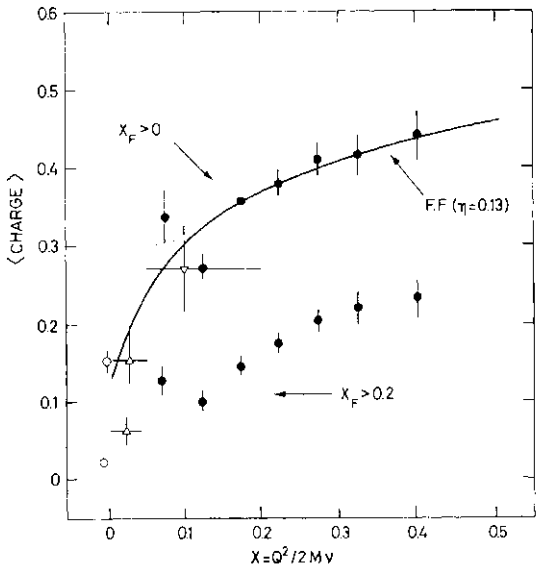

Fig. 30. Mean hadron charge for $x_F>0$, 0.2 versus *x* from Cornell-DESY electroproduction experiment.

difference between the favoured and unfavoured fragmentation function as z-*l is clearly seen from the experimental results.

The same collaboration has also measured the net electric charge of the forward-going hadrons for $x_F>0_9$ which according to the ideas of the *Q-P* model should reflect the charge of the parent quark. In the case of the proton this would be the w-quark (+2/3 charge) for increasing *x*. The mean hadron charge for $x_F>0$ is plotted in Fig. 30 as a function of $x(=Q^2/2Mv)$ and shows that there is a net rise with *x*. The curve is given by the relation

$$\langle\text{charge}\rangle = \frac{\sum l_j^2[l_j \mp \eta]Q_j(x)}{\sum l_j^2 Q_j(x)}$$

where the summation is over all quark flavours with charge l_a and quark distributions $Qj(x)$ given by Field and Feynman,[46] *rj* is the mean quark charge and the experimentally-determined value **9**=0.13 was used, in agreement with **9**=1/6, the prediction for an SU(2) symmetric sea.

Many other results have been presented to this Conference on the hadronic final states of deep inelastic scattering which have been reviewed in other sessions.[47] The results are in qualitative agreement with present ideas on the quark-parton model. However the $p_{\pm}$ dependence of the hadrons should reflect the $p_{\pm}$ of the quarks which "undress" from the nucléon and subsequently, by the inverse process, £'dress" to produce the final state hadron. At present there is no clear evidence emerging from the data on what are the important parameters among q^2, *x*, x_{F9} *W*, *z* in determining the $p_{\pm}$ distributions, but preliminary attempts have been made by the C.H.I.O. group.[48]

It is clear that inclusive final states will provide sensitive measurements for future tests of Q.C.D. in the region of large Q^2 and *W*.

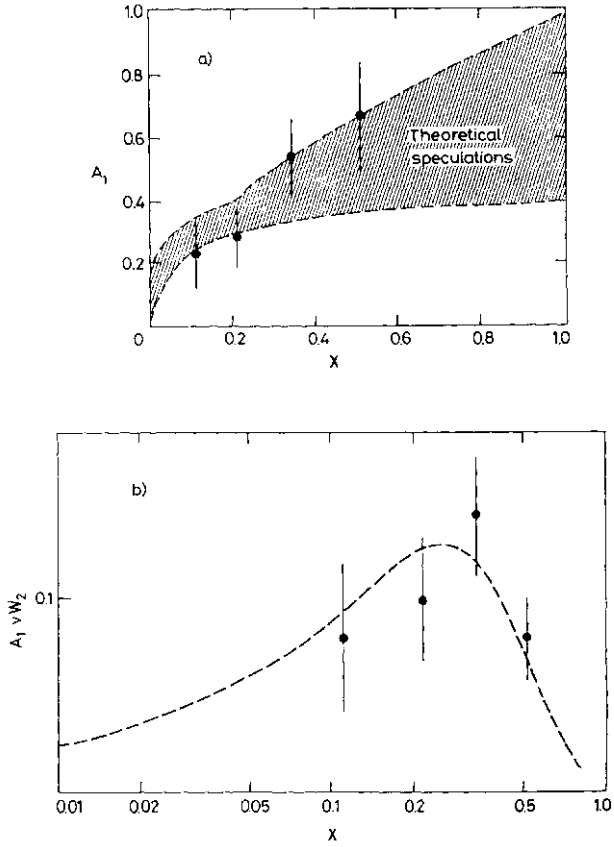

Fig. 31. (a) Asymmetry in scattering polarised electrons off polarised protons from B.S.T.Y. collaboration at SLAC.
(b) $A_1 \nu W_2$ versus x as test of Bjorken sum rule.

§6. Spin Dependent Structure Functions

The study of polarised electrons off polarised protons is according to the simple Quark Parton picture a method of scattering polarised electrons off polarised quarks, and provides information on the additional spin dependent structure functions. The asymmetry for the longitudinal polarisation is given by

$$A = \frac{d\sigma(\uparrow\downarrow) - d\sigma(\uparrow\uparrow)}{d\sigma(\uparrow\downarrow) + d\sigma(\uparrow\uparrow)} \approx K\{A_1 + \eta A_2\}$$

where A_x is related to the difference between the spin 1/2 and spin 3/2 photoabsorption cross-sections and A_2 is related to the transverse longitudinal interference, y is a small kinematic factor and K is a depolarisation factor. The asymmetry is essentially a measure of A_1, which is predicted by the Quark Parton Model to be +5/9 for the proton, whereas for $g^2 = 0$ the asymmetry is negative.[49]

An experiment has been performed by a Bielefeld-SLAC-Tsukuba-Yale Collaboration[50] using a beam of 10^9 e~/sec with a polarisation of 50 %. In order to understand all the systematic errors, an experiment was first made on elastic scattering where the asymmetry is related to the form factors G_E and G_M, and can *be predicted. The measured asymmetry was $A_{xp} = 0.103 \pm 0.015$ ($A_{TH} = 0.\backslash 12 \pm 0.001$) and the relative sign of $G_E \backslash G_M$ was found to be positive. The asymmetry was then measured for inelastic scattering and the results are illustrated in Fig. 31a as a function of x in the range $1 < < 2^2 < 4$ (GeV/c)^2 and $2 < W < 4$ GeV in agreement with the Quark Parton Model. The data are in agreement with a very wide range of theoretical quark-type predictions.[51]

The Biorken sum rule states

$$\int_0^1 \frac{dx}{x} (A_1^p \nu W_2^p - A_1^N \nu W_2^N) = \frac{1}{3} \frac{g_A}{g_V} = 0.417$$

Assuming the $A? = 0$ (Q-P Model), it is possible to check this sum rule approximately from the proton data using a simple scaling extrapolation. The results are illustrated in Fig. 31b and give $\backslash(\grave{a}xlx) A\{\nu Wi = 0M \pm 0S)5$ in good agreement with the predicted value considering the uncertainty in the extrapolation. Data have also been obtained in the resonance region and are consistent with the predicted asymmetry for the different resonance transitions. Future high precision data for deep inelastic scattering should provide very sensitive tests of Q.C.D. effects, in particular at small and large value of x.

§7. Pion and Kaon Form Factors

A determination of the pion and kaon form factors is of interest since it is possible to compare the sizes of the electromagnetic structure of the mesons, and there are many different theoretical predictions based on geometrical models, analyticity and vector dominance. Experimental interest has been stimulated in this field recently by the availability of high-energy high-intensity beams of pions, kaons and even anti-protons using target electrons since the maximum q^2 attainable even for 300 GeV pion and kaon beams is 0.29 (GeV/c)^2 and 0.17 (GeV/c)^2 respectively.

7.1. Pion form factors

The form factors of the pion can be determined by three different methods using space-like and time-like q^2 photons. The precise

measurement of the $\pi\pi$ mass spectrum in e^+e^- storage rings from threshold through the ρ^0 mass region has been made by an Orsay group.[52] Since the two-pion mass spectrum is dominated by the ρ^0 meson close to threshold, they have derived a value of the mean charge radius of the pion which is essentially model-independent of

$$\langle r^2\rangle^{1/2} = 0.678 \pm 0.004 \text{ (stat)} \pm 0.008 \text{ (model) fm.}$$

The electroproduction process $e^-N \to e^-\pi^+N$ has also been used to determine the pion form factor. It has the advantage that it is possible to cover a large range in Q^2 (~10 $(\text{GeV}/c)^2$), but the results are very dependent on the model used to extract the amplitude for the /-channel pion pole term for longitudinally-polarised photons. The following values have been reported for $\langle r^2\rangle^{1/2}$ which are in reasonable agreement with the storage ring determination:

1973 Inverse Electroproduction[53]
0.73±0.13

1976 Electroproduction above Resonance[54]
0.704±0.025

1977 Electroproduction on Resonance[55]
0.74±8:ii

1978 Electroproduction above Resonance[56]
0/711±0.018

It is not clear that given much more precise data on longitudinal and transverse polarisation measurements on pion electroproduction, it will be possible to improve on the uncertainty in the extraction of the form factor from this process.

In principle the measurement of the elastic process $\pi^+e^- \to \pi^+e^-$ provides the most direct method of measuring the pion form factor since

$$\left[\frac{d\sigma}{dq^2}\right]_{el} = \left[\frac{d\sigma}{dQ^2}\right]_{point} |F_\pi(Q^2)|^2$$

The experiments are difficult to perform since the measurements are made in Hydrogen producing very large hadronic backgrounds and the main uncertainty arises from the systematic errors in the experiment.

Measurements have been made using 50 GeV pions at Serpukhov[57] and 100 GeV pions at F.N.A.L.[58] The results of these experiments give for $\langle r_\pi^2\rangle^{1/2}$

1974 $E_\pi = 50$ GeV 0.78 ± 0.10

1977 $E_\pi = 100$ GeV 0.56 ± 0.04

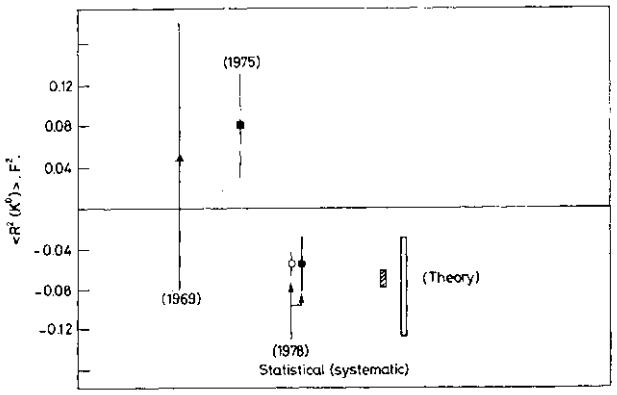

Fig. 32. The K^0 charge radius compared with other experiments. |, Foeth *et al.* (1969); Dydak *et al.* (1975); +, Gsponer *et al.* (1978). The rectangular bars are the theoretical predictions—see text.

An alternative analysis of the first result performed by different authors[59] gave $\langle r^2\rangle = 0.71 \pm 0.05$. It is somewhat disturbing to see such a large difference in these measurements and clearly further measurements are necessary. Theoretical predictions of the mean charge radius in fm are 0.58—0.69 F (V.M.D.),[60] 0.7±0.15 (analyticity)[61] and 0.561 ±0.16 or 0.657±0.15 (geometrical model).[62]

7.2. *Kaon form factor*

The first measurement of the charged kaon form factor has been reported at this conference by the U.C.L.A.-F.N.A.L.-Notre Dame-Pittsburgh group,[63] who have used a 250 GeV K^- beam. Preliminary results from this experiment give $\langle r^2\rangle^{1/2} = 0.51 \pm 0.07$, but at present a comparison with the pion radius is not possible. A theoretical prediction for the kaon radius has been given[62] of 0.520± 0.081 or 0.622±0.068 using the geometrical model and different determinations of the proton radius.

An experiment has been carried out by the Chicago-Wisconsin-SIN group[64] to measure the charge radius of the K^0 meson. This charge can be visualised in the simple non-relativistic quark model, where the *s* and *d* quarks orbit about their centre of mass with the lighter *d* negative quark further out producing a finite negative charge radius. The amplitude of η-regeneration was determined by comparing the rates of coherent regeneration and of diffraction regeneration at $Q^2=0$ using two lead regenerators of very different thicknesses to maximise the coherent signal

and to reduce the correction due to multiple scattering. The results of this very beautiful experiment give

$$\langle r^2(K^0) \rangle = -(0.054 \pm 0.010) \text{ fm}^2$$

Previous measurements[65] of $\langle r^2(K^0) \rangle$ including this new measurement are illustrated in Fig. 32 together with theoretical predictions.[66]

A precise comparison of the charged kaon and pion form factors will require new experimental determinations in the same apparatus where the systematic errors are well understood.

§8. Resonance Production

There are many experimental results in the field of electroporudction and photoproduction in the resonance region $1 < W < 2.5$ GeV.[67] The object of this work is to determine the Q^2 dependence of the electromagnetic couplings of the nucléon resonances in 7-AW*, where many detailed tests of radiative decays of quarks can be tested.

In photoproduction, it is necessary to measure seven quantities in order to determine unambiguously four complex amplitudes (photon ±1-> tar get ±1/2). These consist of the unpolarised differential cross-sections $d\sigma_0$ together with six different kinds of polarisation, *i.e.,* six different asymmetries arising from single and double polarisation measurements *I, P, T, G, H* together with recoil proton polarisation from polarised beam on target.

The most complete set of measurements in this energy range has been made by the Glasgow-Liverpool-Sheffield group at Daresbury,[68] who have measured *da, 2, P, T, G* and *H, le.,* six out of the seven required. Many new measurements on these quantities have been submitted to this conference,[69] as can be seen from Table III on various pion processes, mainly from the different Japanese groups using the Tokyo synchrotron. The major new contribution in electroproduction comes from the total cross-section measurements for polarised beam on polarised target, but other data are now available of various channels. A large amount of new data is available at present and therefore it is important to attempt a complete analysis of all these data from photoproduction and electroproduction in order to determine the Q^2 dependence of the various *yNN** couplings. Following this, it should then be possible to decide which experiments are important and necessary to be carried out.

Table III. Experiments (resonance region).

1. σ_T (pol. proton–pol. target) $W=1200$–2000, $Q^2=0.5, 1.5$			Bielefeld/SLAC/ Tsukuba/Yale
2. $\gamma p \to p\pi^0$			
Σ	0.75–1.31	40°, 50°	Yerevan
T	0.42–1.0	30°, 80°, 105,° 120°	Nagoya/Osaka/Kyoto
P	0.3–1.15	100,° 130°	INS/Tokyo/Sendai/ Kyoto
P	0.83–1.45	60°	Yerevan
P	0.5–0.8	100°, 120°, 140°	Karkov
$d\sigma/d\Omega$	0.6–0.83	130°	INS/Tokyo/Sendai/ Kyoto
$d\sigma/d\Omega$	0.6–1.8	170°	Bonn
3. $\gamma + p \to \pi^+ + n$			
Σ	1.3–1.7	40°, 60°	Yerevan
4. $\gamma + n \to \pi^- + p$			
p	0.7–1.2	60°–100°	Tokyo/KEK/INS
Σ	0.9–1.5	30°–60°	Yerevan
5. *Electroprodn* π^0, γ_l^0			
0°–40°	$Q^2=.15$		Bonn
	$Q^2=0.3$		

§9. The Next Step

The next step will come from experiments which are either approved or have already taken a lot of data, but there are obvious areas of physics where progress should occur.

In photoproduction, charm must surely be seen from the existing large amounts of data which are presently under analysis at the level of ~ 1 ***/ib.*** The emulsion technique works well in what appears to be at first sight a very hostile environment, and with ten times the statistics already available to be measured, tens of charmed events should be found. Once charm has been well proven, then photoproduction is a good process in which to study charmed baryons.

The possibility of studying quark jets through quark pair production in comarison with e^+e^- data should provide important information on the photon structure. In this connection, the use of the nucleus as a "quarkfilter" where the */u, d, X* quarks are absrobed preferentially compared with *c, b, t* quarks is an application where high mass states can be enhanced relative to low mass

states. The measurement of Compton scattering and Compton inelastic scattering at high energies becomes easier and should be able to provide useful information on quark and gluon effects similar to inelastic scattering.

At lower energies, the study of mesons in the 1-3 GeV mass region is still an area of physics which is largely unexplored, but requires special probes, *e.g.*, polarised photons etc. to separate out the complex resonance structures. In the resonance region, the time has surely been reached in both photoproduction and low Q^2 leptoproduction when only specific experiments should be done which are necessary to remove ambiguities in the extraction of the amplitudes. In inelastic lepton scattering, the obvious need is for high precision data over the whole (x, Q^2) plane and its extension to large Q^2, including the separation of proton and neutron structure functions to prove or disprove the very successful Q.C.D. theory. The study of electrons, muons and photons in the final state has very interesting applications in our understanding of different flavours in the small x sea, including a test of quark mass scales through Q^2 dependences. If the present Q.C.D. picture continues to work well, then the study of final states in deep inelastic scattering will provide many interesting tests on the role of the quark in the nucléon and how the quarks dress to form hadrons in comparison with other processes like e^+e^-, Drell-Yan etc. The study of quark and gluon jets will be difficult in the present accelerator energy range, and new techniques for analysing the data will be required.

The study of lepton-quark scattering where the lepton is either charged or neutral (ν) is a very basic process in which to make explicit tests of any model which explains the role of the basic constituents within the nuceon. At this conference, it is now known that through interference certain hadronic final states produced by photon and Z° exchange are the same. High precision experiments can therefore be made using charged lepton and neutrino beams in order to see what, if any, are the differences in the behaviour of the final states, and therefore in the weak and electromagnetic interaction of the quarks. Perhaps by the next Rochester Conference in two years' time there will be one review of all inelastic lepton scattering processes !

Acknowledgements

I would like to thank Professor K. Kondo for his help in preparing this review, Professor M. Konuma and his colleagues of the University of Kyoto and Professor Y. Yamaguchi and his colleagues of the University of Tokyo for their assistance.

References

1. L.N. Hand and R. Marshall: *Proc. 1977 Int. Symp. Lepton and Photon Interactions, (DESY, Hamburg, 1977).*
2. Contributed paper 647, D. O. Caldwell *et al* (1978).
3. D. O. Caldwell *et al:* Phys. Rev. Letters **23** (1969) 1256.
4. E. Gabathuler: *Proc. 6th Int. Symp. Electron and Photon Interactions at High Energies, (Bonn, 1973),* p. 299.
5. S. Michalowski *et ai:* Phys. Rev. Letters **39** (1977) 737.
6. D. O. Caldwell *et al:* Phys. Rev. **D7** (1973) 1362.
7. CH.I.O. Collaboration: T. W. Quirk (private communication) (1978).
8. R. E. Taylor: session B3E (1978).
9. L. N. Hand: *Proc. 1977 Int. Symp. Lepton and Photon Interactions, (DESY, Hamburg, 1977),* p. 426.
10. E. Reya: private communication.
11. Aachen-Bonn-CERN-London-Oxford-Saclay Collaboration: Oxford University preprint (1978).
12. Contributed paper 763, H. L. Anderson *et al.* (1978).
13. O. Nachtmann: Nucl. Phys. **B63** (1973) 237; **B78** (1974) 455.
14. Contributed paper 837, R. C. Bail *et al.* (1978).
15. A. J. Buras: F.N.A.L. (unpublished).
16. J. Ellis and M. K. Gaillard: Nucl. Phys. **B131** (1977) 285.
17. Berkeley-F.N.A.L.-Princeton Collaboration.
18. European Muon Collaboration (NA2) and CERN-Dubna-Munich-Saclay Collaboration (NA4).
19. D. Sivers *et al.:* Phys. Rev. **D13** (1976) 1234.
20. W. Y. Lee: *Proc. 1977 Int. Symp. Lepton and Photon Interactions, (DESY, Hamburg, 1977),* p. 555.
21. Contributed paper, M. Binkley *et al.* (1978).
22. W. Y. Lee: Session B4E **(1978).**
23. Contributed paper 805, Bonn etc. (1978).
24. Contributed paper 974, Bologna etc. (1978).
25. N. Cabibbo and L. Maiani: PAR-LPTHE 78/12 (1978).
26. Contributed paper 439, R. M. Egloff *et al* (1978).

27. C. W. Akerlof *et al:* Phys. Rev. **D 1 4** (1976) 2864.
28. The decay *(j*>-^*n*'*n* ~ **TT**° indicates small admixture of non-strange quarks.
29. Contributed paper 778, D. P. Barber *et al* (1978).
30. Contributed paper 809, Bonn etc. (1978).
31. Contributed paper 439, R. M. Egloff *et al.* (1978).
32. Contributed paper 297, L. A. Aherhs *et al* (1978).
33. Contributed paper 1079, K. Bunnell *et al.* (1978).
34. H. Cheng and T. T. Wu: *Proc. 1971 Int. Symp. Electron and Photon Interactions at High Energies {Cornell University, 1971).*
35. Contributed paoer 297, L. A. Ahrens *et al.* (1978).
36. R. Dixon *et ai:* Phys. Rev. Letters **39** (1977) 516.
37. G. P. Murtas: session B2E (1978).
38. S. Bartalucci *et al. :* DESY 77/59 (1977).
39. Contributed paper 1069, D. Peterson *et al.* (1978).
40. C. Bemporad : *Proc. 1977 Int. Symp. Lepton and Photon Interactions (DESY, Hamburg, 1977),* p. 165.
41. Contributed paper 808, Bonn etc. (1978).
42. Contributed paper 297, L. A. Ahrens *et al.* (1978).
43. Contributed paper 806, Bonn etc. (1978).
44. Contributed paper 1095, G. Drews *et al.* (1978).
45. B. Andersson *et al.:* Nucl. Phys. **B135** (1978) 273; R. D. Field and R. P. Feynman: CALT-68-618 (1977); L. M. Seghal: Proc. 1977 Int. Symp. Lepton and Photon Interactions *(DESY, Hamburg, 1977),* p. 837.
46. R. D. Field and R. P. Feynman: Phys. Rev. **D 1 5** (1977) 2590.
47. P. Sôding: session B3E (1978).
48. R. Wilson: session B3E (1978).
49. S. D. Drell and A. C. Hearn: Phys. Rev. Letters **16** (1966) 908.
50. Contributed paper 686 M. J. Alguard *et al.* (1978).
51. M.J. Alguard *et al.:* SLAC-PUB-2110 (1978) and references therein.
52. J. C. Bizot: private communication.
53. S. F. Berezhnev *et al.:* Sov. J. Nucl. Phys. **16** (1973) 99.
54. C.J. Bebek *et al.:* Phys. Rev. **D 1 3** (1976) 25.
55. G. Bardin *et al:* Nucl. Phys. **B120** (1977) 45.
56. Contributed paper 383, C. J. Bebek *et al.* (1978).
57. G. T. Adylov *et al:* Phys. Letters **53B** (1974) 285.
58. E. B. Daily *et al:* Phys. Rev. Letters **39** (1977) 1176.
59. S. Dubnicka and O. V. Dumbrajs: Phys. Letters **53B** (1974) 285.
60. C. F. Cho and J. J. Sakurai : Lett. Nuovo Cimento **2** (1971) 7.
61. V. Baluni: Phys. Letters **38B** (1972) 535.
62. Contributed paper 1171, T. T. Chou (1978).
63. Contributed paper 857, A. Berevtas *et al.* (1978).
64. Contributed paper 899, A. Gsponer *et al* (1978).
65. H. Foeth *et al:* Phys. Letters **30B** (1969) 276; F. Dydak *et al:* Nucl. Phys. **B102** (1976) 253.
66. N. M. Kroll, T. D. Lee and B. Zumino: Phys. Rev. **157** (1967) 1376; O. W. Greenberg *et al:* Phys. Letters **70B** (1977) 464 and reference therein.
67. R. Marshall: *Proc. 1977 Int. Symp. Lepton and Photon Interactions (DESY, Hamburg, 1977)* p. 489 and references therein.
68. J. R. Holt: private communication.
69. R. Kajikawa: session A4E.

P7a: Neutrino Reactions I—Charged Current Interactions and Multilepton Production

Chairman: M. CONVERSI

Speaker: K. TITTEL

Scientific Secretaries: Y. NAGASHIMA
Y. KOBAYASHI

P7b: Neutrino Reactions II—Neutral Current Interactions and Charm Production

Chairman: D. C. COLLEY

Speaker: C. BALTAY

Scientific Secretaries: H. YUTA
S. KABE

(Tuesday, August 29, 1978; 15: 00-16: 00, 16: 20-17: 20)